

Polymer Library Comprising Fluorene and Carbazole Homo- and Copolymers for Selective Single-Walled Carbon Nanotubes Extraction

Fabien Lemasson,[†] Nicolas Berton,[†] Jana Tittmann,[†] Frank Hennrich,[†] Manfred M. Kappes,^{*,†,‡,§} and Marcel Mayor^{*,†,§,⊥}

[†]Institute for Nanotechnology (INT), Karlsruhe Institute of Technology (KIT), 76021 Karlsruhe, Germany

[‡]Institute of Physical Chemistry, Karlsruhe Institute of Technology, 76021 Karlsruhe, Germany

[§]DFG Center for Functional Nanostructures, 76028 Karlsruhe, Germany

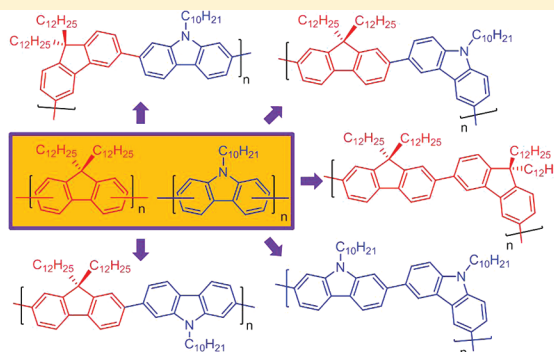
[⊥]Department of Chemistry, University of Basel, 4003 Basel, Switzerland

S Supporting Information

structural variations
polymer library

SWNTs
sorting

structure-property
relationship



ABSTRACT: To date, (n, m) single-walled carbon nanotubes (SWNTs) cannot be selectively synthesized. Therefore, postprocessing of SWNTs including solubilization and sorting is necessary for further applications. Toward this goal, we have synthesized a polymer library consisting of fluorene- and carbazole-based homo- and copolymers. Variations of the connection of these aromatics together with the incorporation of further conjugated monomers give access to a broad diversity of polymers. Their ability to selectively wrap specific (n, m) species is investigated toward HiPco SWNTs raw material which contains more than 40 (n, m) species. Absorption and fluorescence spectroscopies were used to analyze SWNTs/polymer suspensions. These results provide evidence for selective SWNTs/polymer interactions and allow a more detailed assessment of polymer structure–property relationships, thus paving the way toward custom synthesis of polymers for single (n, m) SWNTs extraction.

INTRODUCTION

Single-walled carbon nanotubes (SWNTs) exhibit unique physical and mechanical properties, making them excellent candidates for applications in the fields of optics, electronics, high-strength fibers, and electrolytes.¹ The corresponding raw materials are produced in bulk scale using several different processes including chemical vapor deposition (CVD), laser vaporization, or arc discharge. However, all these methods are not selective in terms of electronic structure type (metallic or semiconducting) or chiral angle (n, m) .² Despite many efforts in this direction, selective synthetic methods yielding monodisperse (n, m) SWNT samples are still not available. As their physical properties are mainly dictated by their chiral angle, postprocessing including sorting of SWNTs is needed to tackle fundamental issues as well as for applications in electronics, optoelectronics, and photonics.³

Any postprocessing approach requires the preparation of SWNT suspensions, either using covalent or noncovalent

functionalization.⁴ The former approach induces defects on the SWNT sidewalls which degrade their physical properties. In the latter approach, the SWNT intrinsic properties remain mainly unchanged due to the preservation of the sp^2 -carbon hybridization of their backbone. This approach was chosen to solubilize SWNTs for enrichment and sorting and several methods were developed for this purpose, which include DNA wrapping followed by ion-exchange chromatography,⁵ solubilization using detergents followed by either dielectrophoresis,⁶ density gradient centrifugation⁷ or nonlinear density gradient centrifugation,⁸ dispersion with small molecules,⁹ or polymer wrapping.¹⁰ Recently, several types of conjugated polymers have been shown to be selective toward a few (n, m) species like poly(9,9-dialkyl-2,7-fluorene) for large chiral angles (close to

Received: August 19, 2011

Revised: December 16, 2011

Published: December 29, 2011

armchair: $\theta \geq 25^\circ$)^{10a,c,h,i} or poly(*N*-decyl-2,7-carbazole) for lower chiral angles (typically $10^\circ \leq \theta \leq 20^\circ$).^{10b} At the same time they also exhibit strong selectivity toward semiconducting SWNTs. This approach is of great interest due to the relatively cheap availability of these materials and due to the perspectives for further improvement thanks to the great variety of structural modifications possible with these types of structures.

Despite numerous studies comprising experimental probes as well as molecular modeling of polymer/SWNT interactions, the reasons for selective solubilization of SWNTs are not fully understood.^{10–12} In order to investigate the correlation between the polymer structures and its SWNT dispersing features, a systematic variation of the polymers structure is desirable. Here we have therefore investigated a small polymer library comprising homo- and copolymers based on 9,9-didodecylfluorene and *N*-alkylcarbazole units connected either in the 2,7 or 3,6 position. The selectivity of these polymers was investigated toward HiPco SWNTs as this material contains more than 40 different (*n*, *m*) tube types ranging from 0.7 to 1.3 nm diameter.¹³ Despite a wide range of parameters able to influence the polymer/SWNT interactions, significant information based on polymeric structural aspect was identified. Although many variables are still not identified, the structural diversity of the library allows to get more insight into specific interactions of polymer/SWNTs and hopefully paves the way toward custom sorting of single (*n*, *m*) species.

RESULTS AND DISCUSSION

Synthesis of Monomers and Polymers. The library comprises four families which include 23 homo- and copolymers stemming from (i) 9,9-didodecyl-2,7-fluorenyl, (ii) 9,9-didodecyl-3,6-fluorenyl, (iii) *N*-alkyl-2,7-carbazolyl, and (iv) *N*-alkyl-3,6-carbazolyl. Additionally, combinations of the aforementioned subunits either with available dihaloareomatics or with themselves completed the collection of copolymers. An overview of the library is given in Table 1. All these conjugated polymers were synthesized by Suzuki coupling, except for polymer **P5** which was synthesized by Yamamoto coupling and polymer **P9** which was assembled by Kumada coupling (Scheme 3). Details of synthetic procedures for monomers and polymers are given in the Supporting Information. The synthesis of several polymers presented in this study has already been reported, namely polymers **P1**,¹⁴ **P7**,^{10b} and **P15–P20**.^{10f}

Yamamoto and Kumada couplings required dihaloareomatics as building blocks, whereas Suzuki cross-coupling required boronic esters and a building block comprising two halides or pseudohalides. Diboronic esters **2**,¹⁵ **4**,^{10b} and **6**¹⁶ were used in this study to access the diversity of the library. They were synthesized by palladium-catalyzed Miyaura borylation of their corresponding dibromides **1**, **3**, and **5**, respectively (Scheme 1). Monoboronic ester **12** (Scheme 2) was synthesized by monolithiation of dibromide **11**¹⁷ followed by quenching with isopropoxy-pinacolborane, yielding monomer **12** in 37% yield. The synthesis of 3,6-dibromofluorene **9** was shortened from five to three steps¹⁸ by starting from the commercially available phenanthrenequinone to access 3,6-dibromo-9,9-didodecylfluorene **10** after alkylation (Scheme 2). Direct reduction of ketone **8** using either hydrazine hydrate¹⁹ or polysiloxane in combination with tris(pentafluorophenyl)borane afforded 3,6-dibromofluorene in good yields. Reduction of ketone **8** using magnesium in dry methanol yields the alcohol.²⁰ Other haloaromatics were commercially available or synthesized according to the literature (see Supporting Information).

For convenience, the yields and molecular weights of the polymers described in this article are summarized in Table 2. Diboronic ester **2**, which displays a 2,7-fluorenyl moiety, was used to synthesize a large part of the library and was reacted in a Suzuki coupling with 11 comonomers to access a variety of polymers. Thus, reaction with its parents 2,7-dibromo-9,9-didodecylfluorene **1** yielded poly(9,9-didodecylfluorene-2,7-diyl) **P1**, in very good yield (99%). Copolymer **P2**, featuring a 2,7 and a 3,6 fluorenyl moiety, was obtained by reaction of diboronic ester **2** with dibromide **10** in very good yield (99%). Strictly alternating copolymers **P6** and **P10**, in which a 2,7 and 3,6 carbazolyl moiety is installed, were synthesized from dibromide **3** and **11** in 98% and 94% yield, respectively. Electron-withdrawing groups such as BTD (benzo-2,1,3-thiadiazole) and anthraquinone were also introduced via their corresponding 4,7-dibromo-2,1,3-benzothiadiazole and 1,5-dichloroanthraquinone to yield polymers **P13** and **P15** in 96% and 80% yields, respectively. Finally, a series of five polyaromatics comonomers were reacted with diboronic ester **2**, namely 1,4-dibromonaphthalene, 1,5-bis(trifluoromethylsulfonyloxy)naphthalene, 1,5-dibromoanthracene, 2,6-dibromoanthracene, and 9,10-dibromoanthracene to access polymers **P23** (90%), **P17** (95%), **P19** (88%), **P21** (94%), and **P22** (88%), respectively.

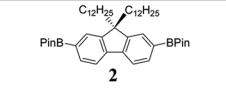
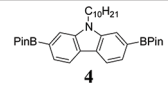
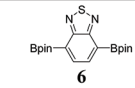
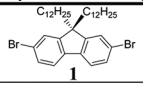
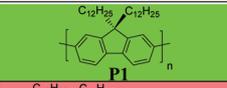
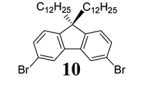
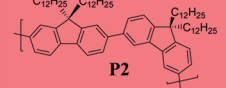
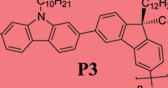
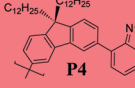
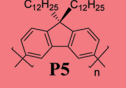
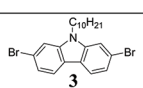
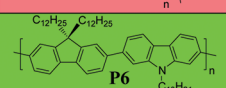
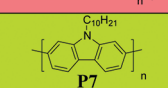
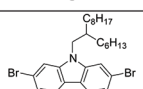
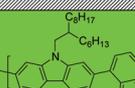
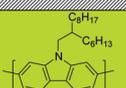
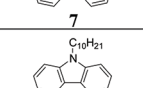
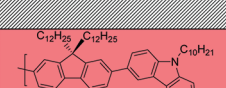
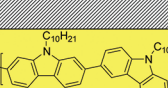
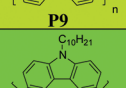
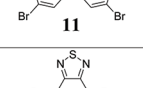
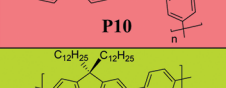
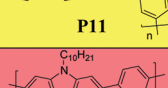
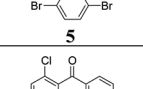
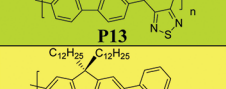
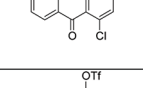
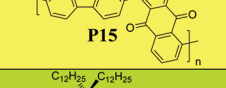
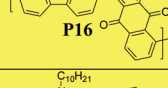
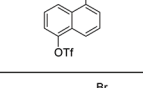
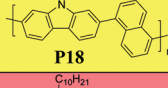
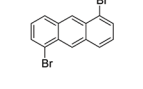
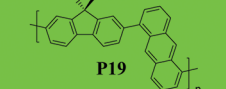
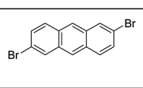
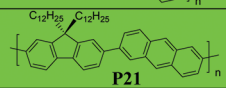
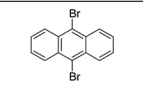
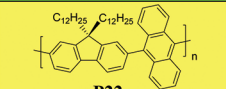
Diboronic ester **4**, displaying a 2,7-carbazolyl moiety, was also reacted in a Suzuki coupling with various (pseudo)haloareomatics to access a large diversity of polymers. Reaction with its parent dibromide **3** yielded poly(*N*-decyl-2,7-carbazole) in **P7** in 76% yield. Polymers **P3** and **P11**, which display a 3,6-fluorenyl and carbazolyl moieties, were obtained from dibromide **10** and **11** in 94 and 89% yield, respectively. The reddish polymer **P14** was synthesized from dibromide **5** in 29% yield. The low yield might be attributed to the low solubility of this polymer. Finally, reaction of diboronic ester **4** with 1,5-dichloroanthraquinone, 1,5-bis(trifluoromethylsulfonyloxy)naphthalene, and 1,5-dibromoanthracene allowed the synthesis of polymers **P16** (39%), **P18** (97%), and **P20** (79%), respectively.

Diboronic ester **6** was reacted first with dibromide **10** to access polymer **P4** (87%) which allowed the introduction of a BTD moiety to a 3,6-fluorenyl moiety. Moreover, the low solubility of polymer **P14** led us to increase the number of carbon atoms in the *N*-alkyl side chain. Thus, diboronic ester **6** was reacted with carbazole **7**, which displays a branched 2-hexyldecyl chain at the carbazole nitrogen atom, to give the reddish polymer **P8** in 76% yield.

Finally, three homopolymers were obtained as follow. A Suzuki coupling of the bifunctional carbazole **12** yielded poly(*N*-decylcarbazole-3,6-diyl) **P12**, and homopolymer **P5** was obtained via Yamamoto homocoupling of its corresponding dibromide **10**. As previously observed for similar 3,6-linked structures, it should be noticed that ¹H NMR spectrum and SEC data of **P5** and **P12** point at the presence of cyclic oligomers within the polymer sample.^{18,21} The first attempt to synthesize polymer **P9** was performed via a Yamamoto coupling of dibromide **7** which yielded high molecular weight polymer **P9** barely soluble in toluene (see Supporting Information). As further investigation of the polymers takes place in toluene, the polymers should be soluble in this solvent. Therefore, dibromide **7** was engaged in a Kumada coupling to yield a lower molecular weight polymer **P9** ($M_n = 1189 \text{ g mol}^{-1}$) which exhibits much higher solubility in common organic solvents including toluene.

Preparation of Polymer/SWNT Dispersions. Dispersions of SWNTs were obtained by sonicating pristine HiPco SWNTs in toluene with an excess of the polymer under investigation.

Table 1. Overview of the Conjugated Polymers Library^a

Boronic (pseudo) esters aryl halides	 2	 4	 6	Homo-coupling
 1	 P1			
 10	 P2	 P3	 P4	 P5
 3	 P6	 P7		
 7			 P8	 P9
 11	 P10	 P11		 P12
 5	 P13	 P14		^a Polymer P12 was synthesized from bifunctional carbazole 12 .
	 P15	 P16		
	 P17	 P18		
	 P19	 P20		
	 P21			
	 P22			
	 P23			

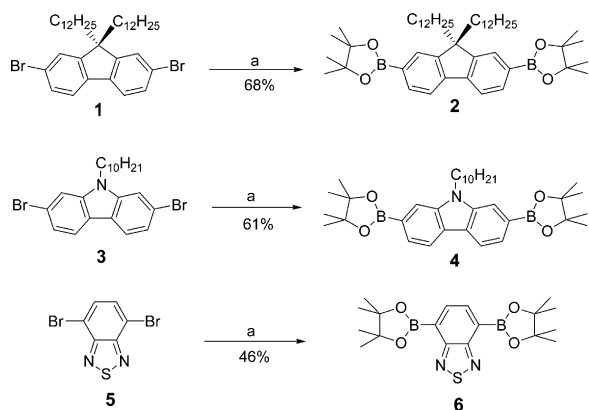
^aPolymers dispersing SWNTs are shaded in green (good), light green (medium), and yellow (poor dispersing properties). Pale red shading indicates that the corresponding suspension was not stable.

Typically, ~1 mg of HiPco SWNTs was added to a solution of 50 mg of the investigated polymer in toluene (15 mL), and the suspension was sonicated for 1 h. Following an established procedure, centrifugation with a mild centripetal acceleration (10 000 rpm, 10 min) was applied to remove large bundles of nanotubes and remaining catalyst particles. A density gradient centrifugation (DGC) was applied to remove the excess polymer and to investigate the possibility of further enrichment.^{10f} The dispersions were analyzed by absorption and photoluminescence–excitation spectroscopy (PLE), allowing the identification and quantification of semiconducting SWNT species (see also Supporting Information).^{13,22}

Dispersing Properties. All recorded PL maps (Figure 1 and Figures S3, S4, S6, and S7) were translated into normalized (see Supporting Information for details concerning the normalizing

procedure) chiral angle (θ) vs diameter (\varnothing) maps in order to visualize the composition of the SWNTs dispersion (Figure 2). The SWNT distribution in HiPco material is represented by sodium cholate dispersions in D₂O, assuming that all SWNT are equally well dispersed in this surfactant. Relative intensity maps of each polymer suspension are also presented in order to allow facile comparison to the original nonuniform distribution of SWNTs in the HiPco material (Figure 3). Relative intensity maps represent the ratio between normalized PL maps and the normalized HiPco SWNTs suspended in D₂O using sodium cholate (i.e., if a polymer disperses all SWNTs equally well, then the relative intensity map would contain only circles with the same diameter). We note that the accuracy of such relative intensity maps is likely to be lower in regions of higher diameters due to the correspondingly low amount of SWNTs present.

Scheme 1. Synthesis of Boronic Esters 2, 4, and 6 Used for the Synthesis of the Polymer Library^a



^aReagents and conditions: (a) PdCl₂(dppf), bis(pinacolato)diboron, dioxane, 80 °C, overnight.

For most of the polymers, the DGC did not allow a significant enrichment of the dispersions and similar PL maps were obtained before and after DGC. Figure 2 presents the chiral angle (θ) vs diameter (\varnothing) maps of these suspensions, and Figure 3 contains their corresponding relative intensities (versus sodium cholate as described in the previous paragraph). However, we observed a clear enhancement of the selectivity caused by DGC for three copolymers comprising a 9,9-didodecyl-2,7-fluorenyl subunit (**P6**, **P13**, and **P23**). The corresponding chiral angle (θ) vs diameter (\varnothing) maps obtained from PL maps before and after DGC treatment are presented in Figure 4.

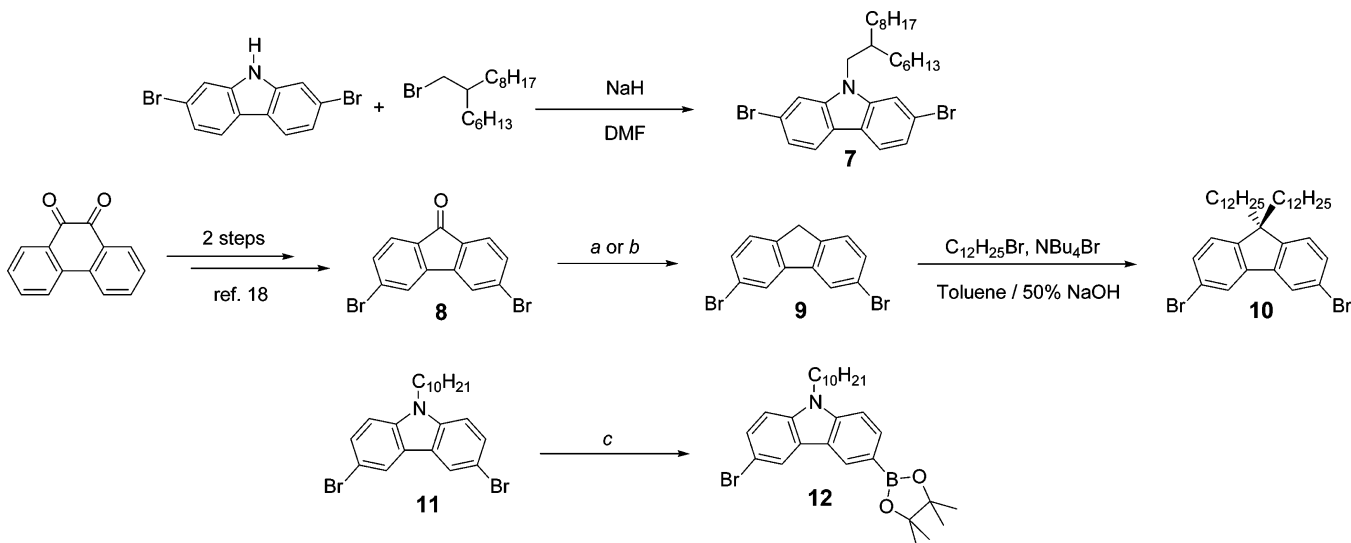
In order to get a qualitative estimate of the SWNT dispersion efficiency of HiPco tubes for each polymer (i.e., how many SWNTs from the parent HiPco mixture are suspended by a polymer regardless to the (n, m) indice), the sum of the intensities of all PL maps peaks attributed to SWNTs (before DGC) was considered. This estimation does not consider any difference in quantum yields of each SWNT as the data required to provide an analysis considering individual quantum yields for each (polymer-wrapped) SWNT type are not available until

now. Thus, the polymers were classified into three categories according to the amount of SWNT (in mg/L) which was dispersed (cf. Table S1 in Supporting Information and related color code in Table 1). Note that this qualitative estimation depends on the parent composition of HiPco tubes. Having a polymer which exclusively selects a (n, m) species which has a low concentration in the starting raw material would lead to a low concentration in the polymer/SWNT suspension. Moreover, this estimation fits fairly well with the absorption spectra of the suspensions displayed in Figure S2. Because of a low signal-to-noise ratio, the absorption spectra of low concentrated suspensions were not displayed.

Finally, some of the reported polymers formed unstable suspensions with SWNTs and precipitation occurred within a few minutes or hours. These polymers, namely **P2–P5**, **P10**, **P14**, and **P20**, were not investigated further.

Polymers Containing a 2,7-Fluorene Moiety. As previously mentioned, poly(2,7-dialkylfluorene)s are known to be extremely selective toward close-to-armchair SWNTs ($\theta > 25^\circ$) and poly(9,9-didodecylfluorene-2,7-diyl) **P1** was found to behave similarly (Figure 2). It should be noticed that the length of the alkyl chains at the C-bridging atom has an influence on the diameter distribution which shifts toward higher diameter tubes. Indeed, the main species in the polymer **P1**/SWNT dispersion is the (7, 6) species, while in comparable conditions (dispersions of HiPco SWNTs in toluene) poly(9,9-dioctylfluorene-2,7-diyl) was reported to mainly disperse the (8, 6) species having a slightly larger diameter.^{10b,c,h} Also, poly(9,9-dihexylfluorene-2,7-diyl) mainly disperses (8, 7) and (9, 7) SWNTs species under similar conditions.^{10c,e} Thus, our results confirm that the diameter of the dispersed nanotubes is inversely proportional to the alkyl chain length, whereas the θ -selectivity is not affected by alkyl chain length variations. This pronounced effect of the length of the alkyl chains of poly(9,9-dialkylfluorene-2,7-diyl) on the diameter selectivity, though not fully understood, is consistent with the predominance of CH/ π interactions between the alkyl chains and the zigzag bonds of the fused hexagons on the nanotubes walls as has recently been suggested by molecular dynamics simulations.^{10b,12} However,

Scheme 2. Synthesis of Monomers 7, 10, and 11^a



^aReagents and conditions: (a) hydrazine monohydrate, KOH, triethylene glycol, 80 °C to reflux, 68%;¹⁹ (b) B(C₆F₅)₃, poly(triethoxysilane), CH₂Cl₂, RT, 67%; (c) *n*-BuLi, isopropoxy-pinacolborane, THF, -78 °C to RT, 37%.

Scheme 3. Overview of the Polymerization Procedures Used in This Study

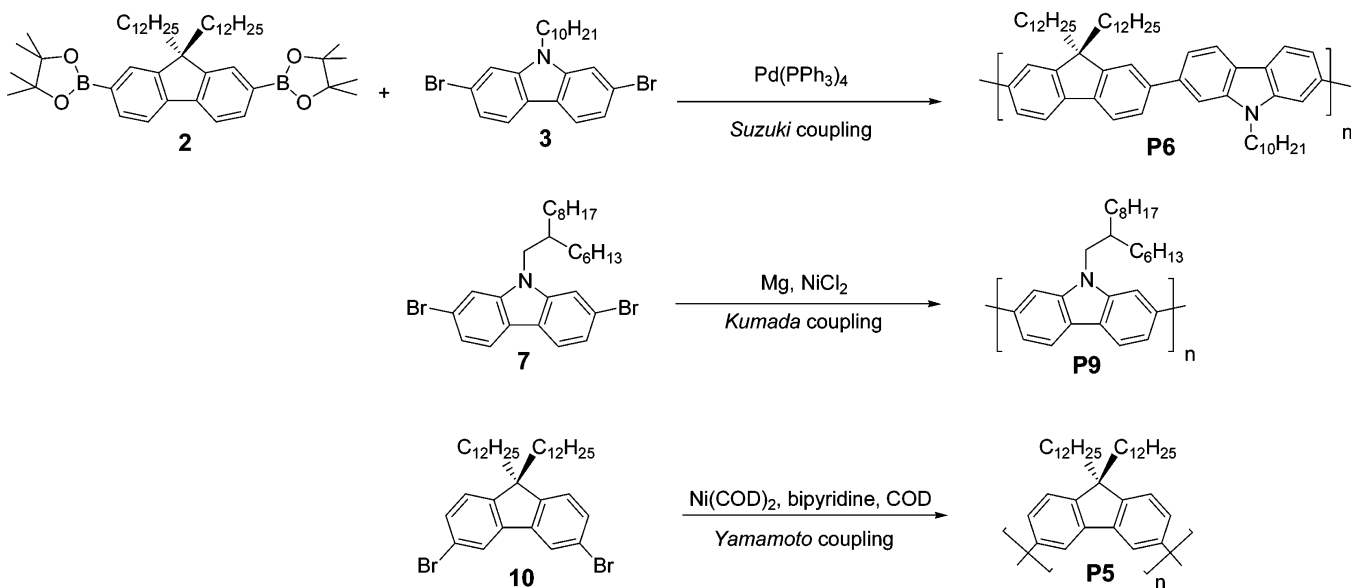


Table 2. Summary of the Synthesis of the Polymers Presented in Table 1 and Used in This Study, Including Yield, Number-Average Molecular Weight, Weight-Average Molecular Weight, and Polydispersity Index

polymer	yield (%)	M_n (Da)	M_w (Da)	PDI	ref
P1	99	12878	53510	4.2	14b
P2	99	8608	14136	1.6	
P3	94	5471	8404	1.5	
P4	87	2350	4760	2.0	
P5	83	11920	66990	5.6	
P6	98	18840	58620	3.1	
P7	20 ^a (76)	3402 ^b	5333 ^b	1.6 ^b	10b
P8	76	17510	50490	2.9	
P9	87 ^c	1189 ^c	1987 ^c	1.7 ^c	
P10	94	10722	19125	1.6	
P11	89	4461	6912	1.6	
P12	98	3035	4552	1.5	
P13	96	29000	58000	2.0	
P14	16 ^a (29)	2250 ^e	2450 ^e	1.1 ^e	
P15	80	11861	25764	2.2	10f
P16	39	2390	3245	1.4	10f
P17	95	59735	220990	3.7	10f
P18	97	23278	133480	5.7	10f
P19	88	21165	51175	2.4	10f
P20	24 ^a (79)	6900 ^e	16800 ^e	2.4 ^e	10f
P21	94	12364	29632	2.4	
P22	38 ^d (88)	17100	24000	1.4	
P23	90	16800	29200	1.7	

^aFraction stemming from Soxhlet extraction with toluene. The percentage in parentheses corresponds to the total yield which comprises a further extraction with chloroform. ^bValue given for the toluene fraction. ^cSynthesized by Kumada coupling. ^dValue given for the chloroform fraction. The percentage in parentheses corresponds to the total yield which comprises a further extraction with toluene. ^eValue given for the toluene fraction which was not fully soluble in THF—the solvent in which the SEC measurement was performed.

it can be noticed that the relative intensities of P1/SWNT dispersion presented in Figure 2 suggests a less pronounced selectivity toward $\theta > 25^\circ$ for $\varnothing > 0.95$ nm. Besides its sorting

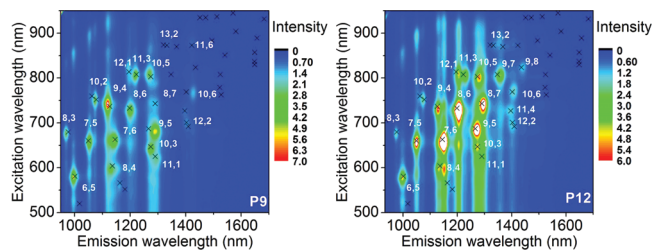


Figure 1. Representative PLE maps of HiPco SWNTs suspensions prepared from polymers P9 and P12 in toluene which allow the identification of each semiconducting (n, m) species. These maps are translated into θ/\varnothing maps allowing an overview of diameter and chiral index selectivity (Figure 2).

properties, polymer P1 is also estimated to have good dispersion efficiency (cf. Table S1).

Changing the selectivity of poly(2,7-fluorene) can be achieved by introduction of aromatic moieties in the polymer main chain. Indeed, polymer P19 exhibits strong diameter selectivity toward SWNTs having $\varnothing > 0.95$ nm, which corresponds to a minor fraction in the starting HiPco material (Figures 2 and 3).^{10f} In contrast, there is no significant chiral angle selectivity: the dispersed SWNTs chiral angles θ range from close to zigzag (12, 1) to armchair (8, 7). Despite the dispersion of only a minor fraction of HiPco nanotubes, polymer P19 yields high concentrations of SWNTs in suspension with regards to the other polymers; i.e., it disperses very efficiently large diameter SWNTs (cf. Table S1). Similar but not so pronounced selectivity properties were observed for polymer P15 having an electron-poor 1,5-anthraquinone moiety in the polymer backbone (Figure 2). Its relative intensity map indicates affinity for high diameter SWNTs (Figure 3). However, the dispersion ability of polymer P15 is much lower than that of polymer P19. Noteworthy is that SWNTs with $\theta < 10^\circ$ were not selected. Introduction of a 1,5-naphthyl moiety as in polymer P17 did not lead to pronounced diameter selectivity. Structural selectivity is directed toward close-to-armchair SWNTs motifs (Figures 2 and 3). The dispersion ability of P17 is also reduced compared with polymer P19. The anthracene connectivity of polymer P19 was varied from 1,5 to 2,6 and 9,10 positions leading to

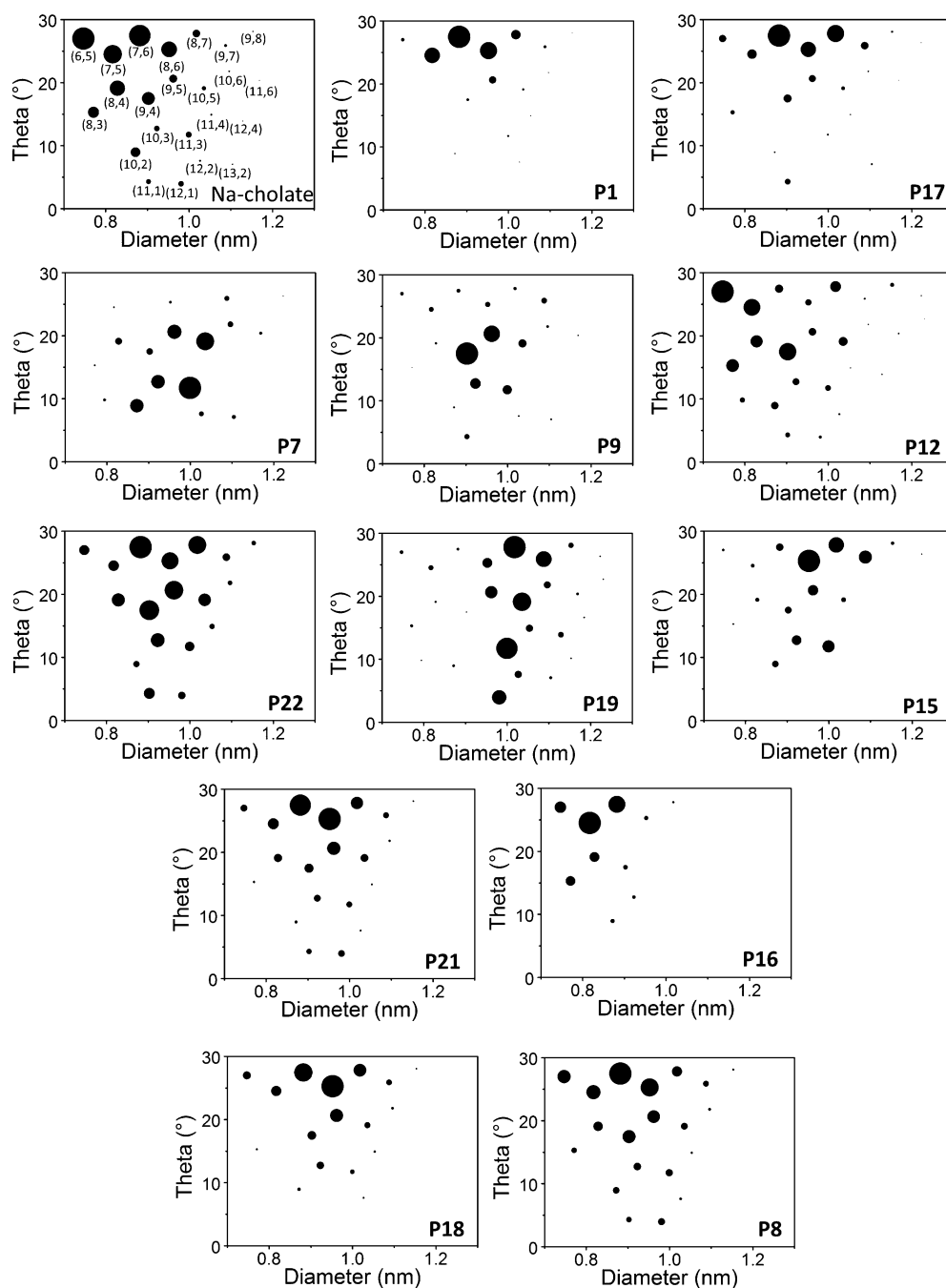


Figure 2. Normalized θ/\varnothing maps of HiPco SWNTs dispersed in aqueous solution using sodium cholate compared to HiPco SWNTs dispersed in toluene using the polymers of this study (after DGC) (see Table 1). Within an individual θ/\varnothing map, the circles areas are proportional to the concentration of the corresponding SWNT species in this dispersion. In the sodium cholate map (top left), the circles are assigned to the (n, m) indices of the corresponding SWNT.

polymers **P21** and **P22**, respectively. Neither of these two polymers is efficient at dispersing SWNTs having $\varnothing < 0.85$ nm (Figures 2 and 3). The suspension stemming from polymer **P22** is relatively more concentrated in low chiral index SWNTs compared to polymer **P21**/SWNTs dispersions. However, polymer **P22** exhibits poor overall solubilizing properties compared with polymer **P21**. Neither of them exhibits a diameter selectivity as pronounced as observed with the parent polymer **P19**.

Polymers Containing a 3,6-Fluorene Moiety. One major observation of these results stems from the family of polymers containing 3,6-fluorenyl units. Whereas polymers derived from 9,9-dialkyl-2,7-fluorene units show good to outstanding dispersing

properties and high wrapping selectivity, all homologous polymers containing 9,9-dialkyl-3,6-fluorenes, namely **P2–P5**, yield unstable suspensions with SWNTs precipitating within minutes. Such behavior demonstrates that the 3,6-connectivity prevents SWNTs dispersion, which can in turn be attributed to an unfavorable polymer conformation that does not enable efficient wrapping of the nanotubes. An analogous unfavorable conformation has been proposed in the case of foldamers which are able to reversibly suspend and release SWNTs by adopting a different conformation by tuning solvent polarity.²³

Polymers Containing a 2,7-Carbazole Moiety. While poly(9,9-didodecylfluorene-2,7-diyl) **P1** exhibits selectivity

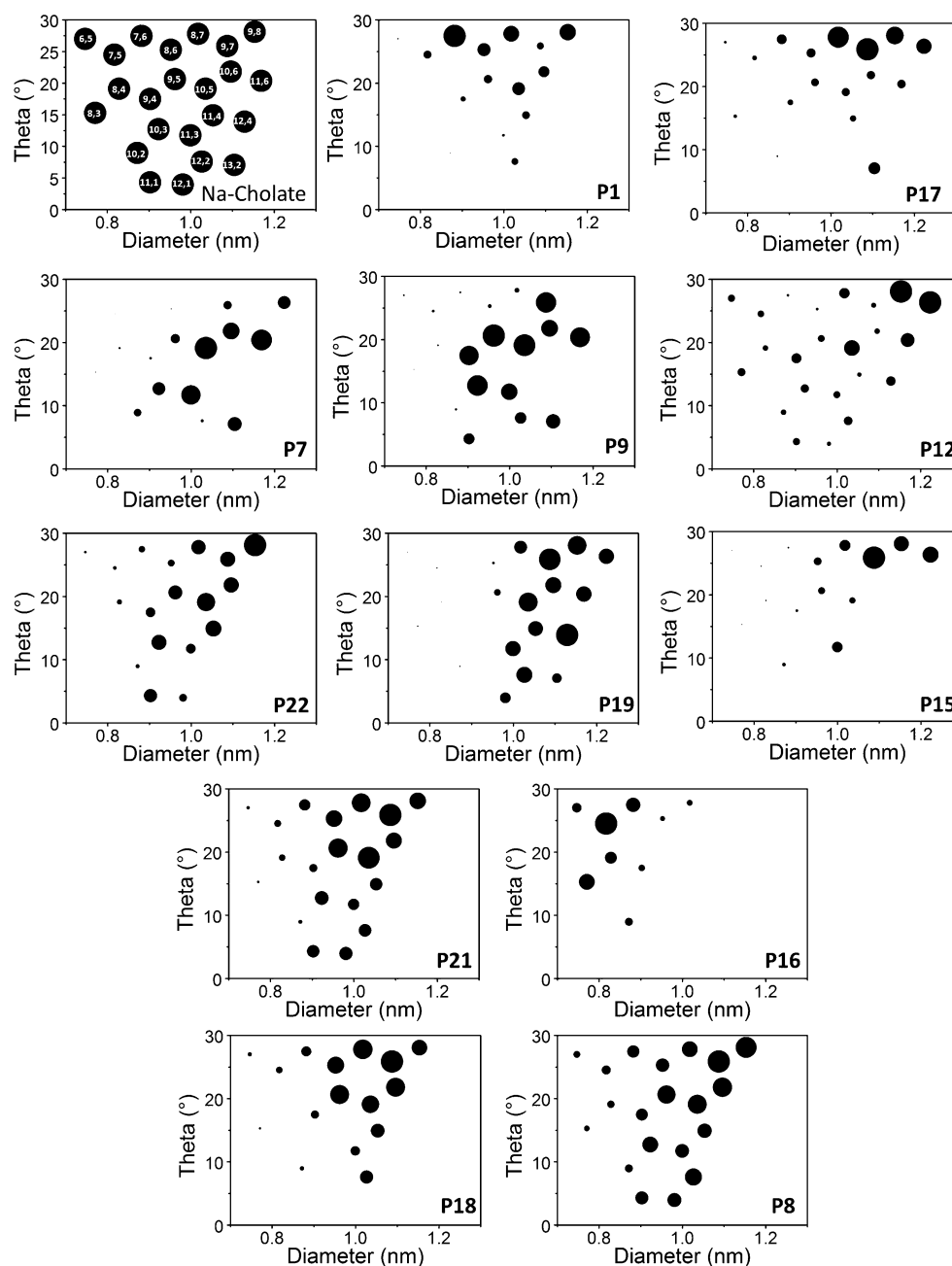


Figure 3. θ/\varnothing maps presenting normalized relative intensities of HiPco SWNTs dispersed in toluene using the polymers of this study (after DGC). Intensities are relative to those of the same (n, m) SWNT species in sodium cholate/water dispersion.

toward high chiral angle SWNTs, its structural proxy poly(*N*-decylcarbazole-2,7-diyl) **P7** exhibits selectivity for lower chiral angles, namely between $10^\circ < \theta < 20^\circ$, making both polymers nicely complementary.^{10b} Another noticeable difference is the dispersing efficiency which was estimated to be 5 times lower in the case of polymer **P7** compared to polymer **P1**. This can be attributed to the single linear alkyl chain attached at the N atom of the carbazole moiety. A way to increase its dispersing efficiency is to introduce a branched alkyl chain at the N atom, yielding poly(*N*-2-hexyldecylcarbazole-2,7-diyl) **P9**. Indeed, the dispersing efficiency is then estimated to increase by a factor of 2. Polymer **P9** exhibits selectivity features relatively similar to those of its parent poly(2,7-carbazole) **P7** despite the increased bulkiness of the side chain (Figures 1–3). Note that polymer **P7** disperses mainly the (11, 3) and (10, 5) species, while polymer

P9 selects preferentially (9, 4) and (9, 5) SWNTs, which represents a slight shift toward smaller diameters and higher θ values (around 20°). Thus, as observed for poly(9,9-dialkylfluorene)s, the nature of the alkyl chain only slightly influences the selectivity. As previously postulated and simulated, the selectivity for lower chiral indices may arise from the sp^2 hybridization of the N-bridging atom which reduces the steric hindrance at this position, thus allowing a tighter complex with the SWNT than the poly(9,9-dialkyl-2,7-fluorene)s which have a sterically more demanding sp^3 -hybridized C-bridging atom.^{10b}

The low solubility of copolymer **P14** did not allow us to test its dispersing properties toward SWNTs (*vide supra*). The introduction of a branched alkyl chain at the N atom of the carbazole moiety afforded the more soluble polymer **P8**, and its dispersing properties toward HiPco SWNTs were tested.

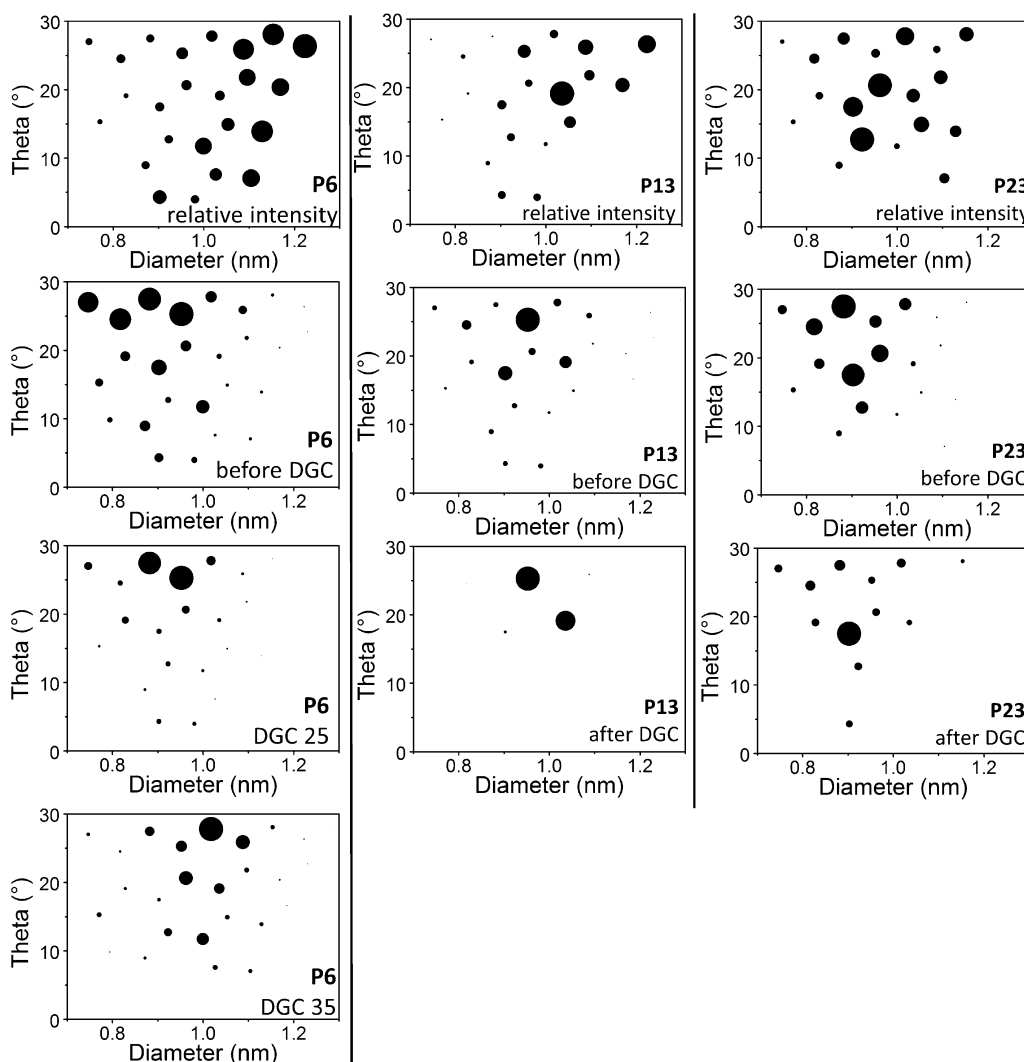


Figure 4. Normalized θ/\varnothing maps of HiPco SWNTs dispersed in toluene using polymers **P6**, **P13**, and **P23** before DGC (second row). First row: normalized relative intensity θ/\varnothing maps corresponding to the second row. Third and fourth row: normalized θ/\varnothing maps after DGC. In the case of polymer **P6**, DGC fractions 25 and 35 are presented due to an inhomogeneous enrichment along the DGC tube, in contrast to suspensions arising from polymers **P13** and **P23** which exhibit homogeneous enrichment.

P8 was found to disperse most SWNTs species, regardless of the diameter and chiral angle, with the (7, 6) and (8, 6) nanotubes dominating the distribution (Figure 2). The θ/\varnothing map representing the relative intensities of SWNTs dispersed by polymer **P8** shows a tendency to suspend SWNTs of higher diameter regardless of the chiral angle (Figure 3). Furthermore, polymer **P8** exhibits high dispersion efficiency.

Copolymers **P16** and **P18** which contain a 2,7-carbazole moiety do not exhibit the same trend and their selectivity is mainly driven by the 1,5-linked anthraquinone and naphthalene groups respectively, as previously reported.^{10f} Indeed, polymer **P16** is selective toward small diameter SWNTs having $\varnothing < 0.9$ nm (Figures 2 and 3) but shows extremely low dispersing efficiency. Polymer **P18** dominantly disperses high chiral indices $\theta > 25^\circ$ with only a minor fraction of $\theta < 25^\circ$. Part of this effect may also be attributable to the HiPco SWNT distribution as shown by the related relative intensity θ/\varnothing map (Figure 3). Even though polymer **P18** yields higher concentration of SWNTs than polymer **P16**, it is not an efficient dispersing agent.

Polymers Containing a 3,6-Carbazole. As shown in Figures 1 and 2, poly(*N*-decylcarbazole-3,6-diyl) **P12** is able to

disperse SWNTs, in contrast to its poly(3,6-fluorene) homologue **P5**. However, no strong selectivity was observed as **P12** disperses most of the nanotubes species initially present and exhibits a θ/\varnothing map similar to the one obtained for sodium cholate aqueous dispersions. The corresponding relative intensity θ/\varnothing map confirms this behavior while also underlining that large diameter SWNTs are well dispersed. Moreover, polymer **P12** shows excellent dispersing efficiency (cf. Table S1). The other mixed polymeric structures **P10** and **P11**, both having a 3,6-linked carbazole subunit in their backbone, yielded unstable suspensions of SWNTs, thus showing behavior similar to their 3,6-fluorene homologues **P2** and **P3**. It should be pointed out that **P11**/SWNTs suspensions are slightly more stable and precipitated within a few hours instead of minutes, thus allowing fluorescence measurements to be recorded. Although the intensity was relatively low, the PL map indicated selectivity toward $\theta \geq 15^\circ$ and diameters ≥ 0.9 nm (Figure S7).

Enhancement Induced by DGC: Polymers P6, P13, and P23. In most cases the polymer wrapping is not that uniform that further fractionation by DGC is possible. However, in the case of the polymers **P6**, **P13**, and **P23**, besides their

intrinsic wrapping selectivity (*vide infra*), a clear enhancement caused by DGC treatment was observed (Figure 4). Copolymer **P6**, which possesses strictly alternating 2,7-linked fluorene and carbazole moieties, is an interesting example of a combination of wrapping selectivities. Given the complementary selectivity of poly(9,9-dialkylfluorene-2,7-diyl) and poly(*N*-alkylcarbazole-2,7-diyl) toward high- and low-chiral angle SWNTs, respectively, it was expected that **P6** would combine both properties. Indeed, as evidenced from the θ/\emptyset map of **P6**/SWNT dispersion in toluene before DGC (Figure 4), the dispersion of a wide range of SWNTs was observed. This tendency is slightly attenuated in the relative intensity θ/\emptyset map which shows the preferential solubilization of higher diameter SWNTs together with the absence of θ sorting (Figure 4). Moreover, the dispersion efficiency of polymer **P6** is high. Interestingly, a post-DGC inhomogeneous enrichment effect was found in this system by harvesting/analyzing discrete fractions within the density gradient. In particular, DGC fraction 25 was enriched with SWNTs having $\theta \geq 25^\circ$, mainly the (7, 6) and (8, 6) species, whereas DGC fraction 35 showed diameter-selective features with $\emptyset \geq 1.0$ nm. The corresponding evolution of the SWNTs distribution—reflecting characteristic buoyant density differences—was further confirmed by absorbance spectrometry (Figure S5). Thus, the nanotubes having the biggest diameter move to higher (= lower density) regions within the density gradient than do smaller nanotubes. The opposite trend has been observed for aqueous dispersions of SWNTs using sodium cholate, where DGC-induced diameter sorting results in smaller-diameter SWNTs settling out at higher points in the centrifuge tube.^{4a} This indicates that in the case of **P6** the polymer coating strongly influences the density of the polymer/SWNT complexes. Note that in most other cases of polymer/SWNTs dispersions studied here we did not find analogous enrichment effects via DGC, possibly because of nonuniform coating of the polymer on the SWNT.^{10f} In contrast, the coating density of polymer **P6** on SWNTs might be relatively uniform for each single (*n, m*) species and vary significantly from one species to another, leading to the differentiation of the buoyant coefficients for polymer/SWNTs complexes, depending upon diameter/*(n, m)* characteristics.

BTD-containing copolymer **P13** showed reduced dispersion efficiency compared to copolymer **P8**. Copolymer **P13** leads to a suspension in which (8, 6) nanotubes are predominant, with a noticeable amount of (9, 4) and (10, 5) as well as other tubes (Figure 4). In this case, applying DGC to the dispersion resulted in a highly enriched suspension of (8, 6) and (10, 5) tubes. All other species, in particular the (9, 4) tube, were efficiently removed during the DGC step. An opposite trend was observed by replacing the electron-deficient BTD unit in copolymer **P13** by a naphthalene unit in polymer **P23**. Polymer **23** did not show significant sorting properties before DGC. However, the relative intensity map indicates the preferential dispersion of smaller diameter SWNTs (Figure 4). Moreover, after DGC treatment the relative amount of the (9, 4) tubes dramatically increased compared to the other tubes, which might indicate specific interactions between polymer **P23** and the (9, 4) tube. It is worth noting that energy transfer is observed in the case of the low-band-gap polymer **P13** (Figure S6). Indeed, we attributed the PL signals observed at excitation wavelength around 500 nm (corresponding to the absorption onset of polymer **P13**, Figure S8) with emission wavelength at around 1200 and 1280 nm, corresponding to the (8, 6) and (10, 5) tubes to energy transfers from the polymer to the corresponding tubes.²⁴

Further features stemming from similar energy transfer were not observed, probably due to the PL analysis window which is out of the absorption region of the described polymers.

CONCLUSION

We have synthesized a polymer library comprising conjugated homopolymers and strictly alternating copolymers based on fluorene and carbazole groups in which their connectivity was varied in either 2,7- or 3,6-positions. The selectivity of these polymers toward specific (*n, m*) SWNTs was investigated with HiPco material containing more than 40 different nanotube species. The dispersing properties were estimated from optical absorption spectra and from photoluminescence intensities, allowing to classify the polymers into three categories depending upon their dispersing efficiency. An indirect correlation between dispersing efficiency and selectivity is observed due to somewhat inhomogeneous distribution of (*n, m*) species in the raw material. Exceptions are polymer **P19**, which shows high concentrated suspensions despite the low “availability” of SWNTs having $\emptyset > 0.95$ nm in raw HiPco material, and polymers **P16**, **P18**, and **P22**, which show low dispersion efficiency despite selecting tubes of high availability.

The trends observed in the SWNTs dispersing features with this polymer library can be summarized as follows: (a) In contrast to the stable suspensions formed with 2,7-connected fluorenyl and/or carbazolyl, SWNTs dispersions derived from polymers containing 3,6-connected building blocks exhibited rapid precipitation of the SWNTs, with the noticeable exception of poly(*N*-decyl-3,6-carbazole) **P12** which efficiently disperses all (*n, m*) SWNTs species. (b) While poly(9,9-didodecylfluorene-2,7-diyl) **P1** is selective toward high chiral angle-SWNTs ($\theta > 20^\circ$), poly(*N*-alkyl-2,7-carbazole) **P7** and **P9** show a strong preference toward SWNTs with $10^\circ < \theta < 20^\circ$. Interestingly, this trend was not affected by the increased bulkiness of the *N*-alkyl side chain of poly(2,7-carbazole), which confirms that the sp^2 hybridization at the N atom may be the origin of the difference in selectivity with poly(9,9-dialkyl-2,7-fluorene). However, the dispersing efficiency was strongly improved, which can be attributed to the enhanced solubility of the polymer. (c) The behavior of alternating fluorene- and carbazole-based copolymers toward SWNTs can be tuned via the chemical nature and connectivity of the subunits. In particular, efficient diameter sorting is achieved by introducing 1,5-linked anthracene units (polymer **P19**). (d) Although in most cases DGC has no impact on the selectivity, DGC-induced separation of SWNTs was observed for some of the copolymers comprising 9,9-didodecylfluorene-2,7-diyl subunits. In particular, DGC fraction-dependent SWNT compositions were observed for copolymers **P6**, **P13**, and **P23**.

This study provides valuable information on structure–property relationships of conjugated homo- and copolymers featuring 2,7- and 3,6-fluorenyl and carbazolyl building blocks—in particular, as pertaining to their interactions with semi-conducting SWNTs. Fine tuning of comonomers allowed a high degree of enrichment in terms of (*n, m*) species as well as in terms of diameters. Ultimately, we expect such studies to pave the way toward custom polymer design for comprehensive direct extraction of single species of SWNTs corresponding to the requirements for specific applications in electronics, optoelectronics, or photonics.

In spite of the systematic structural variation within the (co)polymer libraries of this and other recent studies, clear design rules for a polymer to be able to enrich a particular (*n, m*)

SWNT species still remain to be established. On the experimental side, we are currently investigating structural aspects like the peripheral alkyl chain or the backbone composition of the polymer in further detail. At the same time we hope that our present study will stimulate further computational modeling of polymer wrapping of semiconducting (and metallic) SWNTs.

■ ASSOCIATED CONTENT

■ Supporting Information

Experimental section containing synthetic procedures and characterization of monomers and polymers, description of the preparation and characterization of polymer/SWNTs dispersions, and additional PL maps. This material is available free of charge via the Internet at <http://pubs.acs.org>.

■ AUTHOR INFORMATION

Corresponding Author

*E-mail: marcel.mayor@unibas.ch (M.M.); manfred.kappes@kit.edu (M.M.K.).

■ ACKNOWLEDGMENTS

We thank Peter Gerstel and Christopher Barner-Kowollik for size exclusion chromatography measurements. We also acknowledge ongoing generous support by the DFG Center for Functional Nanostructures (CFN), by the Helmholtz Programme POF NanoMikro, by the Karlsruhe Institute of Technology (KIT), and by the University of Basel.

■ REFERENCES

- (1) (a) Reich, S.; Thomsen, C.; Maultzsch, J. *Carbon Nanotubes: Basic Concepts and Physical Properties*; Wiley-VCH: Weinheim, 2004. (b) O'Connell, M. J. *Carbon Nanotubes: Properties and Applications*; CRC Press Taylor & Francis Group: Boca Raton, FL, 2006. (c) Ajayan, P. M. *Chem. Rev.* **1999**, *99*, 1787–1799. (d) Moniruzzaman, M.; Winey, K. I. *Macromolecules* **2006**, *39*, 5194–5205. (e) Ryu, S.; Lee, Y.; Hwang, J.-W.; Hong, S.; Kim, C.; Park, T. G.; Lee, H.; Hong, S. H. *Adv. Mater.* **2011**, *23*, 1971–1975.
- (2) Joselevich, E.; Dai, H.; Lui, J.; Hata, K.; Windle, A. H. In *Carbon Nanotubes*; Jorio, A., Dresselhaus, G., Dresselhaus, M. S., Eds.; Topics in Applied Physics, Vol. 111; Springer: Berlin, 2008; pp 101–104.
- (3) (a) Martel, R. *ACS Nano* **2008**, *2*, 2195–2199. (b) Adam, E.; Aguirre, C. M.; Marty, L.; St-Antoine, B. C.; Meunier, F.; Desjardins, P.; Ménard, D.; Martel, R. *Nano Lett.* **2008**, *8*, 2351–2355. (c) Cao, Q.; Kim, H. S.; Pimparkar, N.; Kulkarni, J. P.; Wang, C.; Shim, M.; Roy, K.; Alam, M. A.; Rogers, J. A. *Nature* **2008**, *454*, 495–500. (d) Xia, F.; Steiner, M.; Lin, Y. M.; Avouris, P. *Nature Nanotechnol.* **2008**, *3*, 609–613. (e) Holt, J. M.; Ferguson, A. J.; Kopidakis, N.; Larsen, B. A.; Bult, J.; Rumbles, G.; Blackburn, J. L. *Nano Lett.* **2010**, *10*, 4627–4633.
- (4) (a) Hersam, M. C. *Nature Nanotechnol.* **2008**, *3*, 387–394. (b) Komatsu, N.; Wang, F. *Materials* **2010**, *3*, 3818–3844.
- (5) (a) Tu, X.; Manohar, S.; Jagota, A.; Zheng, M. *Nature* **2009**, *460*, 250–253. (b) Zheng, M.; Semke, E. D. *J. Am. Chem. Soc.* **2007**, *129*, 6084–6085.
- (6) Krupke, R.; Hennrich, F.; von Loehneysen, H.; Kappes, M. M. *Science* **2003**, *301*, 344–347.
- (7) Arnold, M. S.; Green, A. A.; Hulvat, J. F.; Stupp, S. I.; Hersam, M. C. *Nature Nanotechnol.* **2006**, *1*, 60–65.
- (8) Gosh, S.; Bachilo, S. M.; Weisman, R. B. *Nature Nanotechnol.* **2010**, *5*, 443–450.
- (9) (a) Peng, X.; Komatsu, N.; Bhattacharya, S.; Shimawaki, T.; Aonuma, S.; Kimura, T.; Asuka, A. *Nature Nanotechnol.* **2007**, *2*, 361–365. (b) Wang, F.; Matsuda, K.; Mustafizur Rahman, A. F. M.; Peng, X.; Kimura, T.; Komatsu, N. *J. Am. Chem. Soc.* **2010**, *132*, 10876–10881. (c) Rahman, A. S. F. M.; Wang, F.; Matsuda, K.; Kimura, T.; Komatsu, N. *Chem. Sci.* **2011**, *2*, 862–867. (d) Marquis, R.; Greco, C.;

Sadokierska, I.; Lebedkin, S.; Kappes, M. M.; Michel, T.; Alvarez, L.; Sauvajol, J.-L.; Meunier, S.; Mioskowski, C. *Nano Lett.* **2008**, *8*, 1830–1835.

(10) (a) Stürzl, N.; Hennrich, F.; Lebedkin, S.; Kappes, M. M. *J. Phys. Chem. C* **2009**, *113*, 14628–14632. (b) Lemasson, F. A.; Strunk, T.; Gerstel, P.; Hennrich, F.; Lebedkin, S.; Barner-Kowollik, C.; Wenzel, W.; Kappes, M. M.; Mayor, M. *J. Am. Chem. Soc.* **2011**, *133*, 652–655. (c) Hwang, J.-Y.; Nish, A.; Doig, J.; Douven, S.; Chen, C. W.; Chen, L.-C.; Nicholas, R. J. *J. Am. Chem. Soc.* **2008**, *130*, 3543–3553. (d) Cheng, F.; Imin, P.; Maunders, C.; Botton, G.; Adronov, A. *Macromolecules* **2008**, *41*, 2304–2308. (e) Nish, A.; Hwang, J.-Y.; Doig, J.; Nicholas, R. J. *Nature Nanotechnol.* **2007**, *2*, 640–646. (f) Berton, N.; Lemasson, F.; Tittmann, J.; Stürzl, N.; Hennrich, F.; Kappes, M. M.; Mayor, M. *Chem. Mater.* **2011**, *23*, 2237–2249. (g) Ozawa, H.; Fujigaya, T.; Song, S.; Suh, H.; Nakashima, N. *Chem. Lett.* **2011**, *40*, 470–472. (h) Chen, F.; Wang, B.; Chen, Y.; Li, L.-J. *Nano Lett.* **2007**, *7*, 3013–3017. (i) Wang, W. Z.; Li, W. F.; Pan, X. Y.; Li, C. M.; Li, L.-J.; Mu, Y. G.; Rogers, J. A.; Chan-Park, M. B. *Adv. Funct. Mater.* **2011**, *21*, 1643–1651.

(11) Star, A.; Stoddart, J. F.; Steuerman, D.; Diehl, M.; Boukai, A.; Wong, E. W.; Yang, X.; Chung, S. W.; Choi, H.; Heath, J. R. *Angew. Chem., Int. Ed.* **2001**, *40*, 1721–1725. Kang, Y. K.; Lee, O. S.; Deria, P.; Kim, S. H.; Park, T. H.; Bonnell, D. A.; Saven, J. G.; Therien, M. J. *Nano Lett.* **2009**, *9*, 1414–1418. Caddeo, C.; Melis, C.; Colombo, L.; Mattoni, A. *J. Phys. Chem. C* **2010**, *114*, 21109–21113.

(12) (a) Ozawa, H.; Fujigaya, T.; Niidome, Y.; Hotta, N.; Fujiki, M.; Nakashima, N. *J. Am. Chem. Soc.* **2011**, *133*, 2651–2657. (b) Gao, J.; Loi, M. A.; de Carvalho, E. J. F.; dos Santos, M. C. *ACS Nano* **2011**, *5*, 3993–3999.

(13) Bachilo, S. M.; Strano, S. M.; Kittrell, C.; Hauge, R. H.; Smalley, R. E.; Weisman, R. B. *Science* **2002**, *298*, 2361–2366.

(14) (a) Teetsov, J.; Fox, M. A. *J. Mater. Chem.* **1999**, *9*, 2117–2122. (b) Lemasson, F.; Tittmann, J.; Hennrich, F.; Stürzl, N.; Malik, S.; Kappes, M. M.; Mayor, M. *Chem. Commun.* **2011**, *47*, 7428–7430.

(15) Utsa, H.; Facchetti, A.; Marks, T. J. *Org. Lett.* **2008**, *10*, 1385–1388.

(16) Zhang, M.; Tsao, H. N.; Pisula, W.; Yang, C.; Mishra, A. K.; Müllen, K. *J. Am. Chem. Soc.* **2007**, *129*, 3472–3473.

(17) Zhang, Z.-B.; Fujiki, M.; Tang, H.-Z.; Motonaga, M.; Torimitsu, K. *Macromolecules* **2002**, *35*, 1988–1990.

(18) Fomina, N.; Hogen-Esch, T. E. *Macromolecules* **2008**, *41*, 3765–3768.

(19) During this study, the following publication appeared where ketone **8** was reduced using hydrazine monohydrate: Song, Y.; Xu, W.; Zhu, D. *Tetrahedron Lett.* **2010**, *51*, 4894–4897.

(20) Khurana, J. M.; Bansal, K.; Pandey, R. R. *Monatsh. Chem.* **2003**, *134*, 1365–1371.

(21) Ostrauskaite, J.; Strohriegel, P. *Macromol. Chem. Phys.* **2003**, *204*, 1713–1718.

(22) Weisman, R. B.; Bachilo, S. M. *Nano Lett.* **2003**, *3*, 1235–1238. Lebedkin, S.; Hennrich, F.; Kiowski, O.; Kappes, M. M. *Phys. Rev. B* **2008**, *77*, 165429.

(23) Zhang, Z.; Che, Y.; Smaldone, R. A.; Xu, M.; Bunes, B. R.; Moore, J. S.; Zang, L. *J. Am. Chem. Soc.* **2010**, *132*, 14113–14117.

(24) Berton, N.; Lemasson, F.; Hennrich, F.; Kappes, M. M.; Mayor, M. Manuscript submitted.